ACCOUNTS
of chemical research

Crystallization Features of Normal Alkanes in Confined Geometry

YUNLAN SU, GUOMING LIU, BAOQUAN XIE, DONGSHENG FU, AND DUJIN WANG*

Beijing National Laboratory for Molecular Sciences, Key Laboratory of Engineering Plastics, Institute of Chemistry, Chinese Academy of Sciences, Beijing 100190, China

RECEIVED ON APRIL 30, 2013

CONSPECTUS

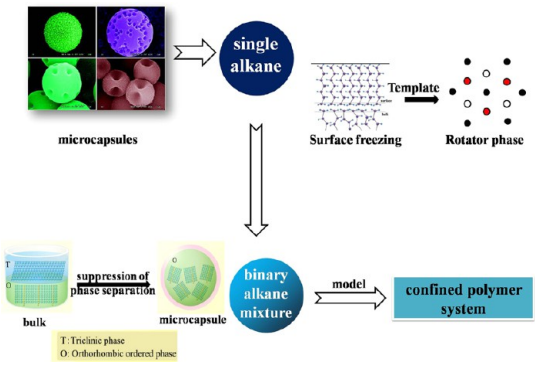

How polymers crystallize can greatly affect their thermal and mechanical properties, which influence the practical applications of these materials. Polymeric materials, such as block copolymers, graft polymers, and polymer blends, have complex molecular structures. Due to the multiple hierarchical structures and different size domains in polymer systems, confined hard environments for polymer crystallization exist widely in these materials. The confined geometry is closely related to both the phase metastability and lifetime of polymer. This affects the phase miscibility, microphase separation, and crystallization behaviors and determines both the performance of polymer materials and how easily these materials can be processed. Furthermore, the size effect of metastable states needs to be clarified in polymers. However, scientists find it difficult to propose a quantitative formula to describe the transition dynamics of metastable states in these complex systems. Normal alkanes [C_nH_{2n+2}, *n*-alkanes], especially linear saturated hydrocarbons, can provide a well-defined model system for studying the complex crystallization behaviors of polymer materials, surfactants, and lipids. Therefore, a deeper investigation of normal alkane phase behavior in confinement will help scientists to understand the crystalline phase transition and ultimate properties of many polymeric materials, especially polyolefins.

In this Account, we provide an in-depth look at the research concerning the confined crystallization behavior of *n*-alkanes and binary mixtures in microcapsules by our laboratory and others. Since 2006, our group has developed a technique for synthesizing nearly monodispersed *n*-alkane containing microcapsules with controllable size and surface porous morphology. We applied an *in situ* polymerization method, using melamine–formaldehyde resin as shell material and nonionic surfactants as emulsifiers. The solid shell of microcapsules can provide a stable three-dimensional (3-D) confining environment. We have studied multiple parameters of these microencapsulated *n*-alkanes, including surface freezing, metastability of the rotator phase, and the phase separation behaviors of *n*-alkane mixtures using differential scanning calorimetry (DSC), temperature-dependent X-ray diffraction (XRD), and variable-temperature solid-state nuclear magnetic resonance (NMR). Our investigations revealed new direct evidence for the existence of surface freezing in microencapsulated *n*-alkanes. By examining the differences among chain packing and nucleation kinetics between bulk alkane solid solutions and their microencapsulated counterparts, we also discovered a mechanism responsible for the formation of a new metastable bulk phase. In addition, we found that confinement suppresses lamellar ordering and longitudinal diffusion, which play an important role in stabilizing the binary *n*-alkane solid solution in microcapsules. Our work also provided new insights into the phase separation of other mixed system, such as waxes, lipids, and polymer blends in confined geometry. These works provide a profound understanding of the relationship between molecular structure and material properties in the context of crystallization and therefore advance our ability to improve applications incorporating polymeric and molecular materials.

1. Introduction

Crystallization performance is an important physicochemical property for polymeric materials, since the crystallinity and superstructural morphology greatly influence thermal and mechanical properties that in turn determine practical applications. Wunderlich has summarized two extreme

Published on the Web 08/15/2013 www.pubs.acs.org/accounts
10.1021/ar400116c

paths of polymer crystal nucleation via metastable phases.[1] In the fast cooling process (intramolecular crystal nucleation) from the melt state, polymer tends to form metastable folded-chain crystals, while the most stable extended-chain crystals can form only in a slow cooling process (intermolecular crystal nucleation).[2] The metastable chain folding is a favorite pathway in the kinetic selections of polymer crystal nucleation. The polymer lamellae form can be regarded as the metastable state in which its thickness increases through several metastable states, each metastable state corresponding to a particular number of folds per chain.[3] There is a broad class of metastable states in polymeric materials, and the metastability is dependent on the microscopic phase size.[4,5] Since it is of great necessity to clarify the size effect of metastable states in polymers, in recent years, considerable attention has been paid to the research of confined crystallization of polymers, which usually occurs in block copolymers, graft polymers, and polymer blends.[6−13] However, it is difficult to be propose a quantitative formula for describing the transition dynamics of metastable states in the crystalline polymeric systems, due to the well-known reasons of polydispersity of molecular weight distribution, side chain architecture, and the existence of multiple hierarchical structures as well as different domain sizes in the polymer system. Normal alkanes [C_nH_{2n+2}, *n*-alkanes], consisting of linear chains of saturated hydrocarbons as the most fundamental organic series and showing molecular weight distribution of integrity and manifest crystalline structures in solid state, can provide well-defined model systems for studying the complex crystallization behaviors of polymer materials, surfactants, lipids, and so forth.[14]

Being such a fundamental and important system, the crystallization behavior of *n*-alkanes has been extensively studied and a plethora of phases occurring between the isotropic liquid and full-crystallization states have been identified.[15−18] Bulk *n*-alkanes have some unique features during the phase transition processes, such as the surface freezing phenomenon,[19−24] rotator phases,[25,26] and odd−even effect in the low-temperature crystalline phases.[18,27] The research on the crystallization behavior of *n*-alkanes in a confined space, in which the amount of surface alkane molecules is dramatically increased with the decrease of the size of confined geometry, can help to detect and understand the precise mechanism of crystallization of *n*-alkanes and the effect of surface freezing on the formation of rotator phases in condensed state. Different kinds of confined spaces, such as one-dimensional[28,29] or two-dimensional[30,31] hard confined spaces and three-dimensional soft confined systems,[32−35] have been considered. However, little work has been done on the crystallization behavior of *n*-alkanes confined in a three-dimensional hard space, for example, in hard shell microcapsules, which can afford a stable confined crystallization environment.

In the past decade, we have been engaged in the investigation of the confined crystallization behavior of single component *n*-alkanes and binary *n*-alkane mixtures in narrow size-distributed microcapsules prepared by an *in situ* polymerization method. Compared with the free *n*-alkane in bulk state, there are three characteristics of phase behaviors of single component and binary mixtures confined in microcapsules: enhancement of surface freezing, the crossover of rotator phase from transient to metastable, and the suppression of phase separation. The study of confined crystallization behaviors of microencapsulated alkanes not only has guiding significance for the polyolefin morphology and crystallography but also provides a new idea for the development of functional polyolefin materials.

2. Preparation of Monodispersed Microcapsules

In order to build a stable and hard three-dimensional confinement, we developed a new synthetic strategy to obtain surface porous microcapsules.[36] Nearly monodispersed microcapsules with controllable surface porous morphology were prepared by *in situ* polymerization of melamine and formaldehyde with the template of nonionic surfactant micelles, and with this method, normal alkanes (from C_{14} to C_{23}) and alkane mixtures can be encapsulated as phase change material. Three types of nonionic surfactants, including Triton X-100 ((4-(1,1,3,3-tetramethylbutyl)phenyl-poly-(ethylene glycol), cloud point T_{cp} = 59 ± 3 °C),[36] NP-10 (polyoxyethylene (10) nonyl phenyl ether, T_{cp} = 65 ± 2 °C),[37] and Tween 80 (polyoxyethylene-20-sorbitan monooleate, T_{cp} = 93 °C),[37] have been tried. Tween series of surfactant emulsifiers are fit for the preparation of microcapsules containing alkanes, the size distribution of which was confirmed to be less monodispersed compared with those prepared with TritonX-100 or NP-10 as emulsifiers. SEM images of two kinds of microcapsules with Triton X-100 and NP-10 as emulsifiers are shown in Figure 1, in which the microcapsules exhibit good monodispersity with an average diameter of ca. 2 μm. The microcapsules display rough surface and possess a large amount of pores on the surface

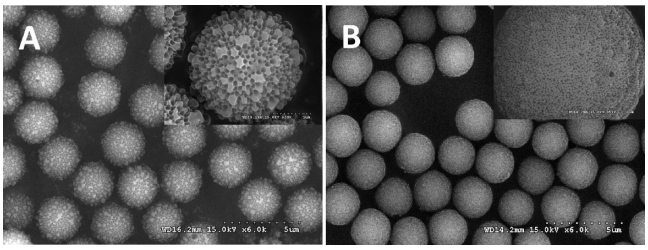

FIGURE 1. SEM images of microcapsules prepared by *in situ* polymerization with Triton X-100 (A) and NP-10 (B) as emulsifier above their cloud point. Panel A reproduced from ref 36. Copyright 2008 American Chemical Society. Panel B reproduced from ref 37 by permission of The Royal Society of Chemistry.

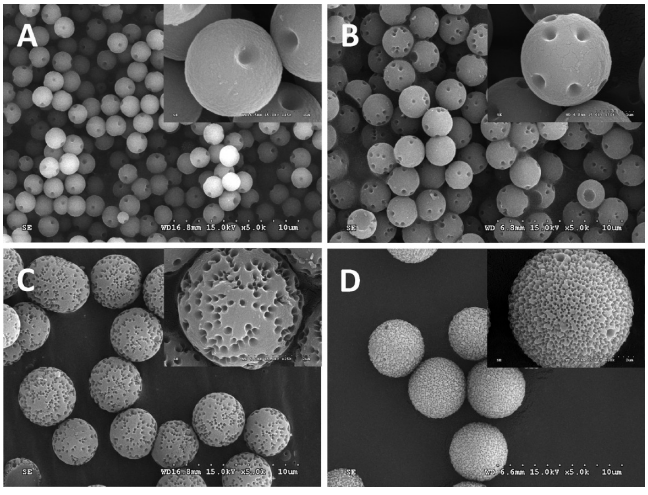

FIGURE 2. SEM images of porous microcapsules prepared by fixing the ratio of core material to shell material at 1:3 and changing the amount of core material: (A) 0.50, (B) 0.67, (C) 1.00, and (D) 1.50 g, respectively. The insets are the high-magnification images. Reproduced from ref 36. Copyright 2008 American Chemical Society.

with pore sizes of ca. 150 or 25 nm, which may be templated by the nonionic surfactant micelles above T_{cp}. The size of the microcapsules (d =1.0−5.0 μm), the pore size (d = 15−400 nm) and pore density can be well-controlled by changing the amount of core material or the ratio of shell material to core material with all the other conditions fixed (as shown in Figure 2). Changing the reaction temperature has also been proven to be an effective way to tune the microcapsule size, surface pore size, and density.[38] The surface porosity can be tuned in the microcapsules prepared both above and below T_{cp} of the nonionic surfactants.

The size distribution plot of microcapsules analyzed by the software (Scion Image for Windows) showed that the dispersion coefficient for the microcapsules is only 0.035.[37] The quite small dispersion coefficient indicates that the microcapsules are nearly monodispersed.[39] In addition, the microcapsule has a typical core−shell structure (as shown

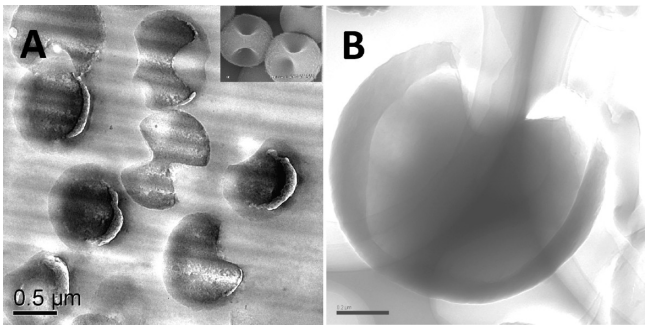

FIGURE 3. TEM images of microcapsule obtained with the amount of core material 0.5 g and the ratio of core material to shell material 2:3. (A) The sample was prepared by the ultramicrotomy method (inset is SEM image of the same sample). (B) The high-magnification TEM image of the microcapsule (scale bar 200 nm). Reproduced from ref 36. Copyright 2008 American Chemical Society.

in Figure 3) with the shell thickness of ca. 100 nm, indicating that the *n*-alkane has been successfully encapsulated into the microcapsules.[36] The monodispersed porous microcapsules with controllable core−shell structure and size can provide an ideal confined inner space for the study of confined crystallization of *n*-alkanes and other small molecules.

3. Enhancement of Surface Freezing

3.1. Single *n*-Alkane Component. The surface crystalline monolayer of normal alkanes has been reported to form at temperatures of up to ∼3 °C above the bulk crystallization temperature and stacks into a planar hexagonal phase. This surface crystallization phenomenon is intimately related to the formation of the bulk rotator phase.[19−22] This kind of peculiar crystallization behavior in *n*-alkanes is probably due to the methyl-end with low surface energy or long chain geometrical form of *n*-alkanes.[23] Another possible reason has also been put forward that surface freezing can be entropically stabilized by fluctuations along the axis of the molecules.[24] The surface freezing phenomenon of *n*-alkanes occurs for chain lengths ranging from $n = 15$ to $n = 50$, which has been widely investigated by X-ray reflectivity, grazing incidence X-ray diffraction (GID), surface tension measurements, ellipsometry, nonlinear optics, Gibbs adsorption isotherm studies, and molecular-dynamics simulations.[19−22] The direct measurement of the surface freezing of *n*-alkanes in hard microcapsules by normal thermal calorimetry was reported by us recently.[40−42] For the microencapsulated *n*-octadecane (*m*-C_{18}) (Figure 4b), the phase change behavior in the heating process is similar to that of bulk *n*-octadecane (C_{18}) (Figure 4a), which is related to the phase transition between a triclinic phase and melt.[41] The phase change behavior of cooling process, however,

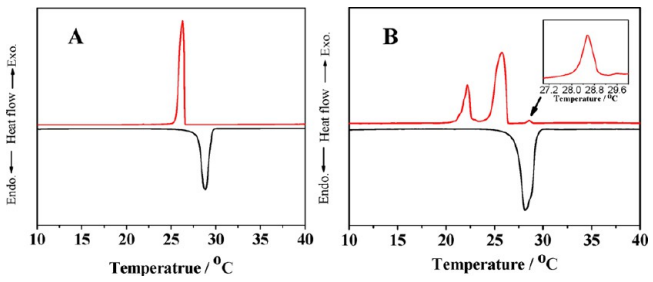

FIGURE 4. DSC traces of *n*-octadecane during the heating and cooling processes: (a) bulk *n*-octadecane; (b) microencapsulated *n*-octadecane. Specimens were heated to 40 °C at a rate of 2 °C/min and then cooled to 0 °C at the same rate, followed by heating again to 50 °C. The first cooling and second heating thermograms were recorded. The insertion in panel b is the magnification of the surfacing freezing peak. Reproduced from ref 41. Copyright 2008 American Chemical Society.

is quite different, in which three exothermic peaks appear. Above the bulk freezing temperature by 3 °C, a small sharp exothermic peak with normal enthalpy (ΔH_s generally smaller than 0.5 J/g) emerges, as shown in the insertion of Figure 4b, corresponding to the surface freezing of *m*-C_{18}. This small peak is assigned to a thermodynamic first-order phase transition, taking the similar result of *n*-hexadecane in emulsified droplets as a reference.[43] The formation of a surface freezing monolayer was directly observed in the DSC measurements, which is attributed to the large specific area provided by the inner wall of the microcapsules. The amount of alkane molecules standing on the core−shell interface of the microcapsule, as calculated to be ca. 1%, is much larger than that on the vapor−liquid interface of bulk alkane, which consequently exerts prominent influence on the crystallization of confined alkanes.

According to Sirota and Ocko,[19,44,45] the surface crystalline monolayer stacks into a planar hexagonal phase similar to the rotator phase, which can be an ideal nucleation site for the bulk crystallization and subsequently induces the formation of bulk rotator phase. The similar structure between the surface freezing phase and rotator phase was verified by variable-temperature solid-state ^{13}C NMR (VT solid-state ^{13}C NMR), a powerful tool for the investigation of phase transition of microencapsulated *n*-docosane.[42] As shown in Figure 5, the NMR signals at 45 °C (surface freezing phase) are similar to those between 43 and 37 °C (rotator phase), implying that the surface freezing phase has a similar structure as the rotator phases.

3.2. Binary *n*-Alkane Mixtures. In the microencapsulated binary *n*-alkane mixtures, the enhancement of surface freezing phenomenon was also observed by DSC similar to the microencapsulated single component *n*-alkane.[46,47] As

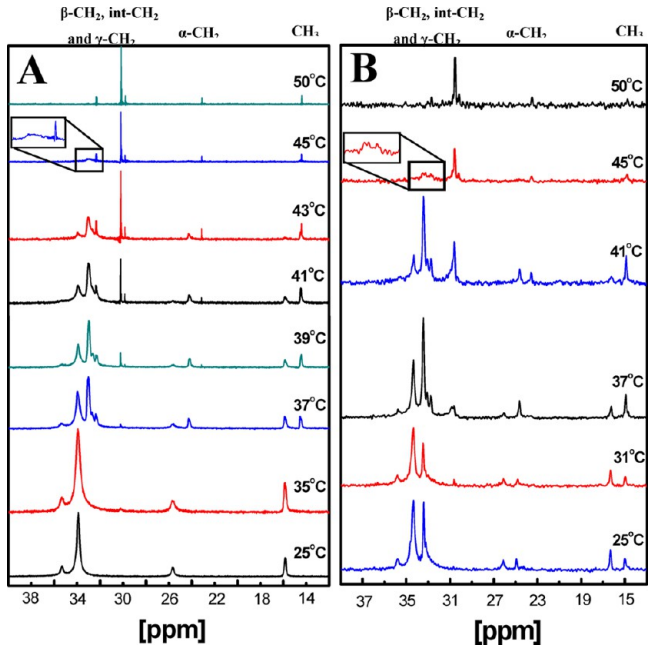

FIGURE 5. Variable-temperature solid-state ^{13}C NMR results of *n*-docosane during the cooling process: (A) bulk sample; (B) microencapsulated sample. The insets are the high-magnification images for the surface freezing phase. Reference 42 — Reproduced by permission of the PCCP Owner Societies.

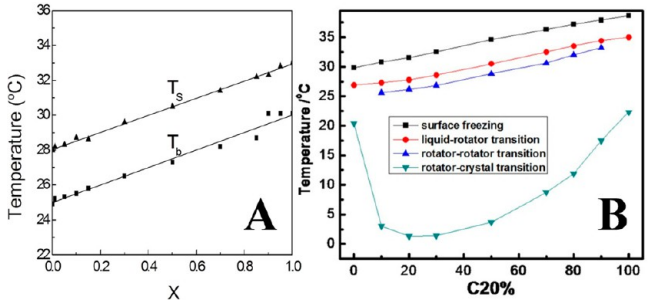

FIGURE 6. (a) The surface freezing temperature (T_s) and bulk freezing temperature (T_b) in *m*-C_{18}/C_{19} as a function of composition (*x* of C_{19}). Reproduced from ref 46. Copyright 2008 American Chemical Society. (b) The relationship between different transition temperatures in *m*-C_{18}/C_{20} system show and the mass fraction of C_{20}, respectively. Reference 47 — Reproduced by permission of the PCCP Owner Societies.

a special crystallization behavior, which emerges at a higher temperature than the freezing point, surface freezing is proven to share the same composition as the bulk mixture when the carbon number difference (Δn) is small (as for $\Delta n = 1$, 2, or 3). For example, a surface freezing monolayer for microencapsulated C_{18}/C_{19} mixture (*m*-C_{18}/C_{19}) was detected by DSC (Figure 6a), which is a mixed homogeneous crystalline phase with continuous change in the composition of the surface layer.[46] The difference in carbon numbers between C_{19} and C_{18} is negligible, so entropic mixing is

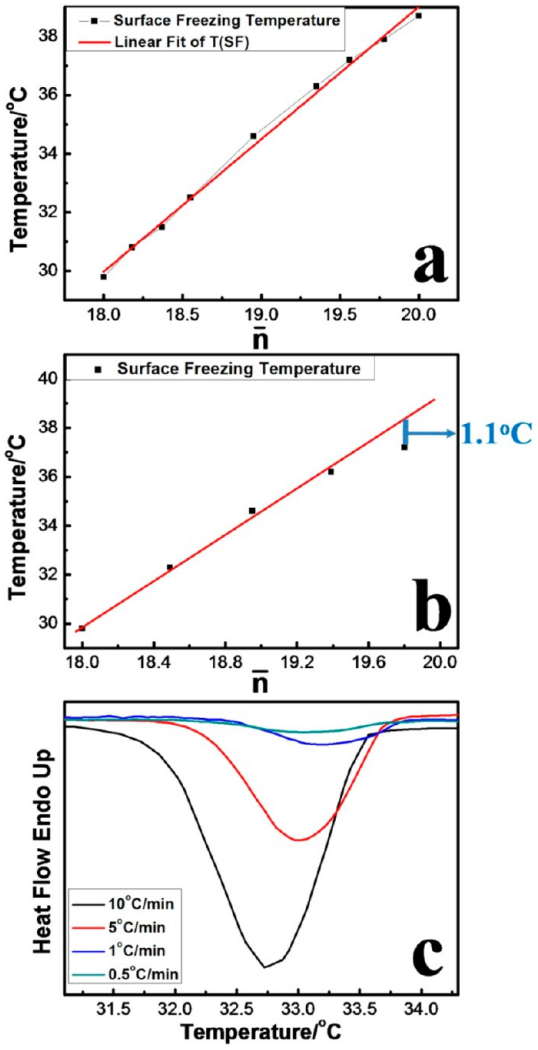

FIGURE 7. Relations between the average chain length ($\bar{n}$) of the binary *n*-alkane mixtures and the surface freezing temperature in microcapsules: (a) the *m*-C_{18}/C_{20} samples under all concentrations; (b) the binary mixtures with various carbon number difference under equal mass fraction of the two components; (c) the DSC traces of the surface freezing phase under different cooling rates. Reproduced from ref 48. Copyright 2012 American Chemical Society.

dominant and a mixed homogeneous crystalline monolayer is favored. For the *m*-C_{18}/C_{20} system, the surface freezing temperature (T_s) also varies continuously and monotonically with the increase of C_{20} content (Figure 6b).[47] When Δn is small ($\Delta n = 1, 2,$ or 3), we substitute the average chain length ($\bar{n}$) of mixtures for the C_{20} content and the similar variance between T_s and $\bar{n}$ was observed (Figure 7a).[48] The linear relationship can be fitted by the equation:

$$T_s = 4.52\bar{n} - 51.34$$

here T_s is the surface freezing temperature, and $\bar{n}$ is the average chain length. When Δn is small, the calculated T_s and experimental values are in good agreement,

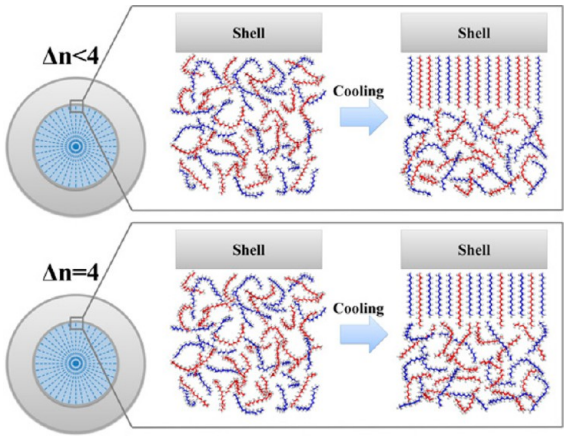

FIGURE 8. Schematic illustration of the crystal structure and interlayer arrangement of surface freezing phase of binary *n*-alkane mixtures with small Δn (1, 2, or 3) and $\Delta n = 4$. Reproduced from ref 48. Copyright 2012 American Chemical Society.

indicating that these samples are composed of well-soluble components. However, the calculated T_s is about 1 °C higher than the experimental one obtained from DSC measurements when $\Delta n = 4$ (Figure 7b). No phase separation was observed in the surface freezing phase because of no division for the surface freezing peak under different cooling rate (Figure 7c).[49] Another reason causing the temperature deviation is probably the composition change in the surface freezing phase of binary *n*-alkane mixtures with large Δn in microcapsules. The CH_3-terminated crystal face with low surface energy is regarded to play a decisive role in the formation of surface freezing phase.[23] Compared with the molecules with the long carbon chain, the short ones will be easily affected by the CH_3-terminated face, since the proportion of CH_3 group in the shorter component is larger than that of the longer one. When the temperature reaches T_s, the molecules on the interface will crystallize, and finally more *n*-alkane molecules with short carbon chain enter into the surface freezing phase, leading to smaller $\bar{n}$ and lower T_s (Figure 8).

4. Crossover of Rotator Phase from Transient to Metastable

4.1. Single *n*-Alkane Component. The rotator phases exist between the isotropic liquid state and the low-temperature stable crystalline phase for single *n*-alkane system. The *gauche* conformation persists in the alkane molecules of the rotator phases, and hence the rotator phase lacks long-range order in the rotational degree of freedom of

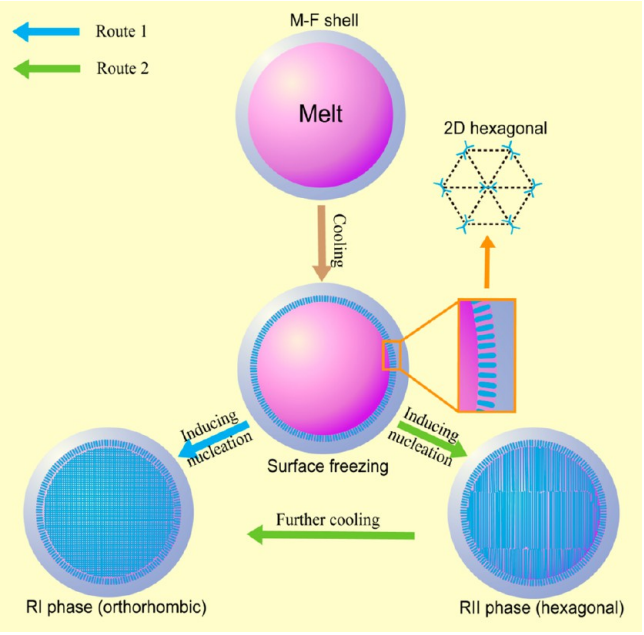

FIGURE 9. Schematic illustration of surface freezing effect on bulk crystallization.

the molecules around their long axis, only exhibiting long-range order in the molecular axis orientation and the center-of-mass position. Five rotator phases, referred to as RI to RV, have been identified by X-ray diffraction experiments and also investigated by calorimetry and have been characterized in terms of side packing, molecular tilt, layer stacking, and azimuthal ordering.[50,51] Odd and even *n*-alkanes show different crystalline forms of the rotator phase because of the different molecular symmetry. The face-centered orthorhombic modification called RI usually occurs in even alkanes C_n (for $n > 20$) as well in odd alkanes C_{11} through C_{25}, while the rhombohedral modification with a hexagonal subcell called RII occurs in even alkanes from C_{22} to C_{26}.[25,26,44] For alkanes, crystal nucleation via mesophases (rotator phase) requires almost no supercooling (<0.05 °C) in bulk. With the increase of chain lengths, as soon as chain folding of polymer starts, a significant supercooling (polyethylene supercools ~20 °C) is required for crystal nucleation.[52,53] The later observation corrected Sirota's earlier idea about the correlation of rotator phase to polymer crystallization.[25] The observed crossover and the fact that short-*n* molecules nucleate into the rotator phase leads us to give serious consideration to the possibility of a metastable hexagonal phase playing a role in nucleating polyethylene.[52]

For even *n*-alkanes in bulk, it is known that the phase diagram contains a crossover from a stable rotator phase (for $n \geq 24$) to a metastable one (for $n = 20, 22$) and then to a transient one (for $n \leq 18$).[25] A number of examples have been described by our group,[40,41] as well as by other authors, that show the crystallization behaviors and rotator phase stability can be strongly affected by the confined geometry. As shown in Figure 9, the formation of a surface freezing monolayer provides ideal nucleation sites and decreases the nucleating barrier of the new rotator phases (RI or RII phase) since the surface freezing monolayer and RII (hexagonal) or RI (pseudohexagonal) have nearly the same in-planar structure. In addition, the lower free energy caused by the enhanced surface freezing makes the transient RI or RII phase stay metastable for a longer time. The specific induction effect of surface freezing phase on the heterogeneous nucleation of melting bulk to RI (route 1) or RII (route 2) phase based on different molecular symmetry of *n*-alkanes in bulk was demonstrated. In the process of route 1, the surface freezing phase directly induces the formation of RI phase. For example, a metastable RI phase has been found in the cooling process of *m*-C_{18} (Figure 4b).[41] In the process of route 2, the surface freezing phase first induces the formation of RII phase and then goes through a RII−RI solid−solid phase transition. A novel metastable RII phase of microencapsulated *n*-nonadecane (*m*-C_{19}) has been found in the cooling process.[40]

A similar metastable rotator phase was found in different confined systems. Ueno[54] measured the crystallization behavior of C_{16} in an oil-in-water emulsion droplet ($d = 0.9\ \mu$m) and observed the orthorhombic rotator phase and 15 °C supercooling after the addition of high melting-point surfactant. The crystallization behavior of C_{16} in miniemulsion ($d =$ 218 nm) showed 16 °C supercooling in the cooling process and 0.7 °C supercooling in the melting process compared with the bulk.[55] In the bulk state of even-numbered alkanes, stable rotator phases no longer exist for $n < 20$. In mesopores, this stability limit is shifted to $n < 14$. For example, the metastable RI has been observed during the cooling process of the mesopore-confined $C_{14}H_{30}$ in Vycor glass.[56] In addition, the metastable RII phase appears in coexistence with the liquid state when $C_{19}H_{40}$ was filled into Vycor glass,[57] which is similar to *m*-C_{19}.[40]

4.2. Binary *n*-Alkane Mixtures. In order to investigate the stability of rotator phase, the temperature region for RII of binary *n*-alkane mixtures (with different Δn) was measured by XRD (Figure 10).[48] Two tendencies are clearly illustrated, the first of which indicates that the larger the Δn, the wider the metastable temperature region of RII is. RII emerges in the mixtures with larger Δn (3 and 4) both in the bulk state

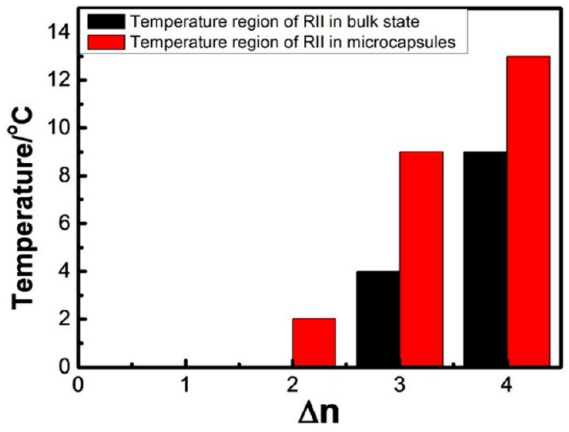

FIGURE 10. Temperature region of RII in the *n*-alkane and binary *n*-alkane mixtures both in the bulk state and in microcapsules. Reproduced from ref 48. Copyright 2012 American Chemical Society.

and in microcapsules. It has been reported that the chain-length mismatch increases a more disordered interlayer interface and thus reduces the interlayer coupling and increases the stability of rotator phase in bulk binary mixtures of different length *n*-alkanes.[58] The other one is referred to the 3D confinement, indicating that once microencapsulated, the metastable temperature region of RII could be greatly enlarged, and even the RII crossovers from transient in the bulk state to metastable in microcapsules emerge (*m*-C_{18}/C_{20}). In *m*-C_{18}/C_{20} mixtures, RII, for the first time, has been observed with no component containing RII phase itself.[47] With the enlargement of Δn for binary *n*-alkane mixtures, the molecular repulsion will be more enhanced, which will significantly suppress the alkane molecules approaching their next-nearest neighbors within the layer.[47] Therefore, the rotator−rotator phase transition from RII to RI is more and more difficult, and RII can be stabilized in a large temperature region, even emerging in the bulk mixtures with larger Δn and microencapsulated mixtures with smaller Δn. When Δn becomes larger, the metastable temperature region of RII is constantly enlarged, showing a growing stability of this rotator phase.

5. Nucleation Mechanisms of *n*-Alkanes in Microcapsules

Many researchers performed careful experimental studies on droplet dispersions (usually in the micrometer range) of alkanes and polymers, in which the nucleation of alkanes in emulsions was first measured by Turnbull and Cormia,[59] followed by Herhold,[60] Montenegro,[32,55] and Kraack.[52] All these studies reported that the crystallization of droplets occurred at much greater supercoolings than in the bulk material, which is usually regarded as an indication of homogeneous nucleation. It is very difficult to clearly demonstrate that homogeneous nucleation has been found in droplets or confined materials. In fact, recent evidence suggests that surface nucleation (although not often recognized in the literature) in clean droplets is more common than bulk homogeneous nucleation in confined polymers.[61−63] Surface nucleation requires lower supercoolings than classic volume homogeneous nucleation, because it is a process characterized by a lower free energy than the more energetically costly process of creating new crystal surfaces inside an microdomain volume.

Two nucleation mechanisms, homogeneous and heterogeneous, exist within different temperature ranges, dominating different kinds of phase transitions of microencapsulated *n*-alkanes.[44] The surface freezing monolayer is preferential and prevalent at the liquid-to-solid transition, which plays a role as a good template for heterogeneous nucleation, inducing the phase transition from the isotropic liquid state to the rotator phase. In this case, the nucleation mechanism is surface-induced heterogeneous. As for the solid-to-solid transition, the surface freezing phase exerts infinitesimal influence on these transitions, and the main origin for heterogeneous nucleation, some impurity, is isolated into some microcapsules, which cannot affect the entire system of the phase transitions of *n*-alkane. Therefore, during the solid−solid phase transitions of the microencapsulated *n*-alkane, heterogeneous nucleation caused by impurity is largely suppressed and homogeneous nucleation becomes dominant, leading to lower transition temperatures and larger supercooling.

6. Suppression of Phase Separation in Binary *n*-Alkane Mixtures

6.1. Odd−Even *n*-Alkane Binary Mixture. For the bulk *n*-alkane mixtures, the phenomenon of solid−solid phase separation can be usually observed in the temperature range of the low temperature ordered phase.[64−66] For the microencapsulated *n*-alkane mixtures, the suitable confinement can be regarded as another important factor that determines the phase separation in addition to the effect of chain-length difference and the composition.

It is a general case that mixing different chain lengths of *n*-alkanes leads to a dramatic influence on the phase behavior, in particular, when even *n*-alkanes are mixed with odd *n*-alkanes. The solid solution of C_{18}/C_{19} = 90/10 fractionates into two phases (triclinic and orthorhombic), while

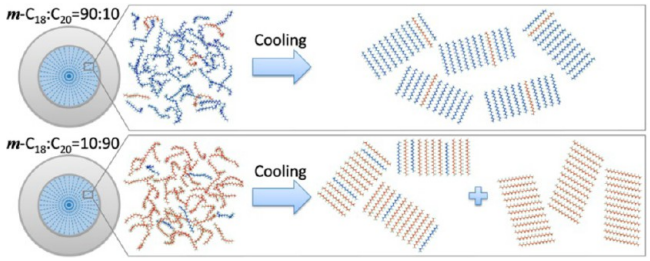

FIGURE 11. Schematic illustration of the crystal structure and interlayer arrangement of *m*-C_{18}/C_{20} = 90/10 (upper part) and *m*-C_{18}/C_{20} = 10/90 (lower part). For *m*-C_{18}/C_{20} = 90/10, the isotropic liquid state is transferred only into orthorhombic ordered phase. For *m*-C_{18}/C_{20} = 10/90, the isotropic liquid state is transferred into the coexistence of triclinic (solely by C_{20}) and orthorhombic ordered phases. Reproduced from ref 68. Copyright 2011 American Chemical Society.

that of *m*-C_{18}/C_{19} = 90/10 only transforms into one stable orthorhombic phase.[67] The solid–solid phase separation of mixed *n*-alkanes, usually observed during the cooling process of bulk samples, is greatly suppressed and even eliminated after being microencapsulated, with the orthorhombic-ordered phase dominating in the low-temperature crystal. For the bulk *n*-alkanes and their mixtures, lamellar ordering has been commonly found in the crystalline state. The absence of (00*l*) reflections in the diffraction patterns of *m*-C_{18}/C_{19} = 90/10 implies positional disordering along the crystallographic *c*-axis (carbon chain). The lamellar ordering and longitudinal diffusion in *m*-C_{18}/C_{19}= 90/10 are suppressed due to the confinement effect.[56]

6.2. Even–Even *n*-Alkane Binary Mixture. Compared with the odd–even system (C_{18}/C_{19}), the even–even *n*-alkane mixture (C_{18}/C_{20}) has a larger chain length difference.[68] Therefore, it is expected that the phase separation will be more enhanced in the bulk state. In bulk, two kinds of phase separation have been observed in compositions of C_{18}/C_{20} = 90/10 and C_{18}/C_{20} = 10/90, resulting in two ordered phases (orthorhombic and triclinic) for the former system and a triclinic ordered phase formed by C_{18} and C_{20} for the latter one.

In microcapsules, the weakening of the layered structure and terminal methyl–methyl interactions due to the confinement plays an important role on suppressing the phase separation between two *n*-alkane components. As shown in Figure 11, the *m*-C_{18}/C_{20} = 90/10 mixture only crystallizes into one stable orthorhombic phase, indicating the total elimination of phase separation. The layered structure of low-temperature crystal phases is partially suppressed similar to *m*-C_{18}/C_{19} system,[67] which further weakens the terminal CH_3–CH_3 interactions, causing the triclinic ordered phase to be more unstable. Therefore, the orthorhombic ordered phase is dominant in *m*-C_{18}/C_{20} = 90/10, eliminating the phase separation originally shown in C_{18}/C_{20} = 90/10. The situation in the *m*-C_{18}/C_{20} = 10/90 mixture, however, is not the same as that in the *m*-C_{18}/C_{20} = 90/10. The triclinic ordered phase (solely by C_{20}) coexists with the orthorhombic ordered phase in *m*-C_{18}/C_{20} = 10/90, showing a partial suppression of the phase separation. Because the small amount of C_{18} cannot strongly disrupt the triclinic crystal lattice of C_{20}, the triclinic ordered phase formed by C_{20} can be preserved. The phase separation is partially suppressed, and two kinds of ordered phases coexist instead of the total separation of the two components in C_{18}/C_{20} = 10/90. Therefore, the different composition (90/10 or 10/90) results in the different relative stability of triclinic and orthorhombic rotator phases, which has a great effect on the final phase separation.

7. Summary and Future Expectations

In summary, microencapsulation can exert a prominent effect on the phase behavior of single *n*-alkane components and binary odd–even and even–even *n*-alkane mixtures. For the microencapsulated single *n*-alkanes and binary mixtures, the surface freezing phenomenon, the observation of metastable rotator phases, and the existing temperature range of rotator phases are all strongly enhanced in the confined space. In addition, the solid–solid phase separation in binary *n*-alkane mixtures is suppressed in confined geometry. A great number of challenges, or opportunities, are still present in this area. First, the sizes of microcapsules prepared at present are at the micrometer scale, which is much larger than the size of *n*-alkane molecules. In-depth understanding of the crystallization behavior of alkanes in nanosized microcapsules should be explored. Preparation of well-defined and stable nanocapsules is still a challenge. Second, the present *in situ* preparation method cannot allow for encapsulating *n*-alkanes with $n > 24$ in the melamine–formaldehyde resin shells, due to the limited emulsification capability of the nonionic surfactants and the lower reactive temperature.

In order to study the confined crystallization behavior of *n*-alkanes with longer chains, nanocomposites of *n*-alkanes with silica nanospheres have been designed and prepared in our group, which can provide a well-defined model for studying the complex crystallization behavior of polymer nanocomposites. Ongoing and future efforts will focus on the understanding of the role of nanometer confined space and interface interaction on the crystallization of *n*-alkane and polymer materials.

We thank the National Natural Science Foundation of China (Grants 51103166 and 21274156) and China National Funds for distinguished Young Scientists (Grant 50925313) for financial support.

BIOGRAPHICAL INFORMATION

Yunlan Su is an associate professor of Key Laboratory of Engineering Plastics at Institute of Chemistry, Chinese Academy of Sciences (ICCAS). She obtained her Ph.D. from Peking University in 2003 and undertook postdoctoral studies with Professor Zhiwu Yu in Tsinghua University from 2004 to 2006. She has been an associate professor at Institute of Chemistry since 2006. Her research is mainly focused on the confined crystallization behavior of *n*-alkanes in microcapsules and on the surface of silica nanospheres.

Guoming Liu is an assistant professor of ICCAS in Beijing. He received his Ph.D. in 2011 from ICCAS under the supervision of Prof. Dujin Wang. His research interests include structure−property relationships of polymers, polymer crystallization and relaxation in confined space, and characterization of solid material structure by X-ray scattering.

Baoxuan Xie obtained his Ph.D. in 2008 from ICCAS under the supervision of Prof. Dujin Wang and started as a postdoctoral associate in the laboratory of Prof. George H. Nancollas at the State University of New York at Buffalo. He joined Prof. Ludmilla Aristilde's group at Department of Biological and Environmental Engineering in Cornell University as postdoctoral associate in 2012. His research interests include synthesis of functional porous microcapsules, biomineralization and biomaterials, confined crystallization of soft materials, and molecular environmental chemodynamics of organic contaminants.

Dongsheng Fu is a faculty member of ICCAS in Beijing. He received his Ph.D. in 2012 from ICCAS under the supervision of Prof. Dujin Wang. His research interests focused on the confined crystallization behavior of *n*-alkanes and alkane mixtures in microcapsules.

Dujin Wang is a professor of ICCAS in Beijing. He received his Ph.D. in 1995 from Peking University under the supervision of Prof. Jinguang Wu. After two years postdoctoral research at ICCAS with Prof. Duanfu Xu, he joined the institute as a faculty member in 1997. In 2000, he was appointed to a professorship at ICCAS. In 2009, he received an award from the National Natural Science Foundation of China for Distinguished Young Scholars. He is currently the director of CAS Key Laboratory of Engineering Plastics and the Deputy Director of ICCAS. His research interests include polymer morphology and processing, crystallization behavior and self-assembly of side chain branched polymers, and confined crystallization of normal alkanes and polymers.

FOOTNOTES

*Corresponding author. E-mail: djwang@iccas.ac.cn. Tel: +86-10-82618533. Fax: +86-10-82618533.

The authors declare no competing financial interest.

REFERENCES

1 Wunderlich, B. Crystal nucleation, growth, annealing. *Macromolecular Physics*; Academic Press: New York, 1976; Vol. 2.

2 Hu, W. B. Intramolecular crystal nucleation. In *Progress in Understanding of Polymer Crystallization*; Reiter, G., Strobl, G. R., Eds.; Lecture Notes in Physics; Springer-Verlag Press: Berlin, 2007; Vol. 714, pp 47−63.

3 Muthukumar, M. Shifting paradigms in polymer crystallization. In *Progress in Understanding of Polymer Crystallization*; Reiter, G., Strobl, G. R., Eds.; Lecture Notes in Physics; Springer-Verlag Press: Berlin, 2007; Vol. 714, pp 1−18.

4 Keller, A.; Cheng, S. Z. D. The role of metastability in polymer phase transitions. *Polymer* **1998**, *39*, 4461–4487.

5 Cheng, S. Z. D.; Zhu, L.; Li, C. Y.; Honigfort, P. S.; Keller, A. Size effect of metastable states on semicrystalline polymer structures and morphologies. *Thermochim. Acta* **1999**, *332*, 105–113.

6 Frensch, H.; Harnischfeger, P.; Jungnickel, B. J. Fractionated crystallization in incompatible polymer blends. In *Multiphase Polymers: Blends and Ionomers*; Utracky, L. A., Weiss, R. A., Eds.; ACS Symposium Series 395; American Chemical Society: Washington, DC, 1989; Chapter 5, pp 101−125.

7 Arnal, M. L.; Matos, M. E.; Morales, R. A.; Santana, O. O.; Müller, A. J. Evaluation of the fractionated crystallization of dispersed polyolefins in a polystyrene matrix. *Macromol. Chem. Phys.* **1998**, *199*, 2275–2298.

8 Loo, Y. L.; Register, R. A.; Ryan, A. J.; Dee, G. T. Polymer crystallization confined in one, two, or three dimensions. *Macromolecules* **2001**, *34*, 8968–8977.

9 Zhu, L.; Cheng, S. Z. D.; Calhoun, B. H.; Ge, Q.; Quirk, R. P.; Thomas, E. L.; Hsiao, B. S.; Yeh, F.; Lotz, B. Crystallization temperature-dependent crystal orientations within nanoscale confined lamellae of a self-assembled crystalline-amorphous diblock copolymer. *J. Am. Chem. Soc.* **2000**, *122*, 5957–5967.

10 Loo, Y. L.; Register, R. A.; Ryan, A. J.; Dee, G. T. Polymer crystallization in 25-nm spheres. *Phys. Rev. Lett.* **2000**, *84*, 4120–4123.

11 Hamley, I. W. Crystallization in block copolymers. *Adv. Polym. Sci.* **1999**, *148*, 113–137.

12 Loo, Y.; Register, A. Crystallization within block copolymer mesophases. In *Developments in Block Copolymer Science and Technology*; Hamley, I. W., Ed.; Wiley Press: New York, 2004.

13 Müller, A. J.; Balsamo, V.; Arnal, M. L. Nucleation and crystallization in diblock and triblock copolymers. *Adv. Polym. Sci.* **2005**, *190*, 1–63.

14 Small, D. M. *The Physical Chemistry of Lipids*; Plenum Press: New York, 1986.

15 Sirota, E. B.; Singer, D. M. Phase transitions among the rotator phases of the normal alkanes. *J. Chem. Phys.* **1993**, *101*, 10873–10882.

16 Sirota, E. B.; King, H. E.; Hughes, G. J.; Wan, W. K. Novel phase behavior in normal alkanes. *Phys. Rev. Lett.* **1992**, *68*, 492–495.

17 Doucet, J.; Denicolo, I.; Craievich, A.; Collet, A. Evidence of a phase transition in the rotator phase of the odd-numbered paraffins $C_{23}H_{48}$ and $C_{25}H_{52}$. *J. Chem. Phys.* **1981**, *75*, 5125–5127.

18 Dirand, M.; Bouroukba, M.; Chevallier, V.; Petitjean, D. Normal alkanes, multialkane synthetic model mixtures, and real petroleum waxes: Crystallographic structures, thermodynamic properties, and crystallization. *J. Chem. Eng. Data* **2002**, *47*, 115–143.

19 Ocko, B. M.; Wu, X. Z.; Sirota, E. B.; Sinha, S. K.; Gang, O.; Deutsch, M. Surface freezing in chain molecules: Normal alkanes. *Phys. Rev. E* **1997**, *55*, 3164–3182.

20 Wu, X. Z.; Ocko, B. M.; Sirota, E. B.; Sinha, S. K.; Deutsch, M.; Cao, B. H.; Kim, M. W. Surface-tension measurements of surface freezing in liquid normal-alkanes. *Science* **1993**, *261*, 1018–1021.

21 Wu, X. Z.; Sirota, E. B.; Sinha, S. K.; Ocko, B. M.; Deutsch, M. Surface crystallization of liquid normal-alkanes. *Phys. Rev. Lett.* **1993**, *70*, 958–961.

22 Wu, X. Z.; Ocko, B. M.; Tang, H.; Sirota, E. B.; Sinha, S. K.; Deutsch, M. Surface freezing in binary-mixtures of alkanes - New phases and phase-transitions. *Phys. Rev. Lett.* **1995**, *75*, 1332–1335.

23 Sirota, E. B.; Wu, X. Z.; Ocko, B. M.; Deutsch, M. What drives the surface freezing in alkanes? *Phys. Rev. Lett.* **1997**, *79*, 531–531.

24 Tkachenko, A. V.; Rabin, Y. Fluctuation-stabilized surface freezing of chain molecules. *Phys. Rev. Lett.* **1996**, *76*, 2527–2530.

25 Sirota, E. B.; Herhold, A. B. Transient phase-induced nucleation. *Science* **1999**, *283*, 529–532.

26 Sirota, E. B.; King, H. E.; Singer, D. M.; Shao, H. H. Rotator phases of the normal alkanes - an X-ray scattering study. *J. Chem. Phys.* **1993**, *98*, 5809–5824.

27 Luth, H.; Nyburg, S. C.; Robinson, P. M.; Scott, H. G. Crystallographic and calorimetric phase studies of n-eicosane, $C_{20}H_{42}$ - n-docosane, $C_{22}H_{46}$ system. *Mol. Cryst. Liq. Cryst.* **1972**, *27*, 337–357.

28 Nanjundiah, K.; Dhinojwala, A. Confinement-induced ordering of alkanes between an elastomer and a solid surface. *Phys. Rev. Lett.* **2005**, *95*, No. 154301.

29 Maeda, N.; Kohonen, M. M. Phase behavior of long-chain n-alkanes at one and between two mica surfaces. *J. Phys. Chem. B* **2001**, *105*, 5906–5913.

30 Knorr, K.; Wallacher, D.; Huber, P.; Soprunyuk, V.; Ackermann, R. Are solidified fillings of mesopores basically bulk-like except for the geometric confinement? *Eur. Phys. J. E* **2003**, *12*, 51–56.

31 Henschel, A.; Hofmann, T.; Huber, P.; Knorr, K. Preferred orientations and stability of medium length n-alkanes solidified in mesoporous silicon. *Phys. Rev. E* **2007**, *75*, No. 021607.

32 Montenegro, R.; Landfester, K. Metastable and stable morphologies during crystallization of alkanes in miniemulsion droplets. *Langmuir* **2003**, *19*, 5996–6003.

33 Kraack, H.; Sirota, E. B.; Deutsch, M. Homogeneous crystal nucleation in short polyethylene. *Polymer* **2001**, *42*, 8225–8233.

34 Gulseren, I.; Coupland, J. N. The effect of emulsifier type and droplet size on phase transitions in emulsified even-numbered n-alkanes. *J. Am. Oil Chem. Soc.* **2007**, *84*, 621–629.

35 Kraack, H.; Sirota, E. B.; Deutsch, M. Measurements of homogeneous nucleation in normal-alkanes. *J. Chem. Phys.* **2000**, *112*, 6873–6885.

36 Xie, B. Q.; Shi, H. F.; Liu, G. M.; Zhou, Y.; Wang, Y.; Zhao, Y.; Wang, D. J. Preparation of surface porous microcapsules templated by self-assembly of nonionic surfactant micelles. *Chem. Mater.* **2008**, *20*, 3099–3104.

37 Liu, G. M.; Xie, B. Q.; Fu, D. S.; Wang, Y.; Fu, Q.; Wang, D. J. Preparation of nearly monodisperse microcapsules with controlled morphology by in situ polymerization of a shell layer. *J. Mater. Chem.* **2009**, *19*, 1–6.

38 Fu, D. S.; Su, Y. L.; Xie, B. Q.; Liu, G. M.; Li, Z. B.; Jiang, K.; Wang, D. J. Pore decoration on microcapsule surface using nonionic surfactant micelles as template: Temperature effect and encapsulation mechanism investigation. *Colloids Surf., A* **2011**, *384*, 219–227.

39 Viau, G.; FievetVincent, F.; Fievet, F. Monodisperse iron-based particles: Precipitation in liquid polyols. *J. Mater. Chem.* **1996**, *6*, 1047–1054.

40 Xie, B. Q.; Shi, H. F.; Jiang, S. C.; Zhao, Y.; Han, C. C.; Xu, D. F.; Wang, D. J. Crystallization behaviors of n-nonadecane in confined space: Observation of metastable phase induced by surface freezing. *J. Phys. Chem. B* **2006**, *110*, 14279–14282.

41 Xie, B. Q.; Liu, G. M.; Jiang, S. C.; Zhao, Y.; Wang, D. J. Crystallization behaviors of n-octadecane in confined space: Crossover of rotator phase from transient to metastable induced by surface freezing. *J. Phys. Chem. B* **2008**, *112*, 13310–13315.

42 Fu, D. S.; Su, Y. L.; Xie, B. Q.; Zhu, H. J.; Liu, G. M.; Wang, D. J. Phase change materials of n-alkane-containing microcapsules: Observation of coexistence of ordered and rotator phases. *Phys. Chem. Chem. Phys.* **2011**, *13*, 2021–2026.

43 Shinohara, Y.; Kawasaki, N.; Ueno, N. S.; Kobayashi, I.; Nakajima, M.; Amemiya, Y. Observation of the transient rotator phase of n-hexadecane in emulsified droplets with time-resolved two-dimensional small- and wide-angle x-ray scattering. *Phys. Rev. Lett.* **2005**, *94*, No. 097801.

44 Sirota, E. B. Supercooling, nucleation, rotator phases, and surface crystallization of n-alkane melts. *Langmuir* **1998**, *14*, 3133–3136.

45 Sloutskin, E.; Sirota, E. B.; Kraack, H.; Ocko, B. M.; Deutsch, M. Surface freezing in n-alkane solutions: The relation to bulk phases. *Phys. Rev. E* **2001**, *64*, No. 031708.

46 Jiang, K.; Su, Y. L.; Xie, B. Q.; Jiang, S. C.; Zhao, Y.; Wang, D. J. Effect of geometrical confinement on the nucleation and crystallization behavior of n-alkane mixtures. *J. Phys. Chem. B* **2008**, *112*, 16485–16489.

47 Fu, D. S.; Liu, Y. F.; Liu, G. M.; Su, Y. L.; Wang, D. J. Confined crystallization of binary n-alkane mixtures: stabilization of a new rotator phase by enhanced surface freezing and weakened intermolecular interactions. *Phys. Chem. Chem. Phys.* **2011**, *13*, 15031–15036.

48 Fu, D. S.; Liu, Y. F.; Gao, X.; Su, Y. L.; Liu, G. M.; Wang, D. J. Binary n-alkane mixtures from total miscibility to phase separation in microcapsules: Enrichment of shorter component in surface freezing and enhanced stability of rotator phases. *J. Phys. Chem. B* **2012**, *116*, 3099–3105.

49 Sloutskin, E.; Wu, X. Z.; Peterson, T. B.; Gang, O.; Ocko, B. M.; Sirota, E. B.; Deutsch, M. Surface freezing in binary mixtures of chain molecules. I. Alkane mixtures. *Phys. Rev. E* **2003**, *68*, No. 031605.

50 Ungar, G. Structure of rotator phases in n-alkanes. *J. Phys. Chem.* **1983**, *87*, 689–695.

51 Ungar, G.; Masic, N. Order in the rotator phase of n-alkanes. *J. Phys. Chem.* **1985**, *89*, 1036–1042.

52 Kraack, H.; Deutsch, M.; Sirota, E. B. n-Alkane homogeneous nucleation: Crossover to polymer behavior. *Macromolecules* **2000**, *33*, 6174–6184.

53 Kraack, H.; Sirota, E. B.; Deuthsch, M. Homogeneous crystal nucleation in short polyethylenes. *Polymer* **2001**, *42*, 8225–8233.

54 Ueno, S.; Hamada, Y.; Sato, K. Controlling polymorphic crystallization of n-alkane crystals in emulsion droplets through interfacial heterogeneous nucleation. *Cryst. Growth Des.* **2003**, *3*, 935–939.

55 Montenegro, R.; Antionetti, M.; Mastai, Y.; Landfester, K. Crystallization in miniemulsion droplets. *J. Phys. Chem. B* **2003**, *107*, 5088–5094.

56 Huber, P.; Soprunyuk, V. P.; Knorr, K. Structural transformations of even-numbered n-alkanes confined in mesopores. *Phys. Rev. E* **2006**, *74*, No. 031610.

57 Huber, P.; Wallacher, D.; Albers, J.; Knorr, K. Quenching of lamellar ordering in an n-alkane embedded in nanopores. *Europhys. Lett.* **2004**, *65*, 351–357.

58 Sirota, E. B.; King, H. E.; Shao, H. H.; Singer, D. M. Rotator phases in mixtures of n-alkanes. *J. Phys. Chem.* **1995**, *99*, 798–804.

59 Turnbull, D.; Cormia, R. L. Kinetics of crystal nucleation in some naomal alkane liquids. *J. Chem. Phys.* **1961**, *34*, 820–831.

60 Herhold, A. B.; King, H. E.; Sirota, E. B. A vanishing nucleation barrier for the n-alkane rotator-to-crystal transformation. *J. Chem. Phys.* **2002**, *116*, 9036–9050.

61 Michell, R. M.; Blaszczyk-Lezak, I.; Mijangos, C.; Müller, A. J. Confinement effects on polymer crystallization: From droplets to alumina nanopores. *Polymer* **2013**, *54*, 4059–4077.

62 Carvalho, J. L.; Dalnoki-Veress, K. Homogeneous bulk, surface, and edge nucleation in crystalline nanodroplets. *Phys. Rev. Lett.* **2010**, *105*, No. 237801.

63 Carvalho, J. L.; Dalnoki-Veress, K. Surface nucleation in the crystallisation of polyethylene droplets. *Eur. Phys. J. E* **2011**, *34*, 1–6.

64 Snyder, R. G.; Clavell-Grunbaum, D.; Strauss, H. L. Spinodal phase separation of unstable solid-state binary n-alkane mixtures. *J. Phys. Chem. B* **2007**, *111*, 13957–13966.

65 Dorset, D. L. Role of symmetry in the formation of normal-paraffin solid-solutions. *Macromolecules* **1987**, *20*, 2782–2788.

66 Dorset, D. L.; Snyder, R. G. Phase separation of a metastable three-component n-paraffin solid solution. *J. Phys. Chem. B* **1999**, *103*, 3282–3286.

67 Jiang, K.; Su, Y. L.; Xie, B. Q.; Men, Y. F.; Wang, D. J. Suppression of the phase separation in binary n-alkane solid solutions by geometrical confinement. *J. Phys. Chem. B* **2009**, *113*, 3269–3272.

68 Fu, D. S.; Liu, Y. F.; Su, Y. L.; Liu, G. M.; Wang, D. J. Crystallization behavior of binary even-even n-alkane mixtures in microcapsules: effect of composition and confined geometry on solid-solid phase separation. *J. Phys. Chem. B* **2011**, *115*, 4632–4638.